JOURNAL OF MATERIALS SCIENCE 8 (1973) 500–508

The microstructure of experimentally deformed limestones

D. J. BARBER
Physics Department, University of Essex, Colchester, Essex

H. R. WENK
Geology Department, University of California, Berkeley, California, USA

The paper presents preliminary results of TEM studies of the microstructure of fine-grained Solnhofen limestone which was deformed in compression experiments at various strain-rates, temperatures and confining pressures. The aims of the tests were to study changes in the patterns of preferred orientation and possible changes in boundaries of the stability fields of the phases, induced by non-hydrostatic stress or large shearing strains. The TEM work on sputter-etched specimens followed extensive investigations by X-ray methods.

Low-temperature deformation (200°C, ~ 26% strain, $\dot{\epsilon} = 10^{-4}$ % sec^{-1}) produces heavily "cold-worked" structures, with many sub-cells containing unresolvable defects. At 300°C the microstructure is slightly less confused: some grains contain only tangles of dislocations while others exhibit ragged deformation bands. At higher temperatures but low strain-rates (600°C, 36% strain, $\dot{\epsilon} = 10^{-6}$ % sec^{-1}) and within the aragonite stability field, the microstructure is more inhomogeneous, with slip and extensive faulting in both the aragonite and the residual calcite grains. Preferred orientation is indicated by significant alignment between fault structures in neighbouring grains. At yet higher temperatures (900°C), twinning still occurs in the calcite but it is less profuse; dislocation densities are generally lower and preferred orientation is weaker, as shown by X-ray results.

1. Introduction

Wenk and Venkitasubramanyan [1] have done an extensive experimental investigation to study changes in preferred orientation of deformed limestone over the stability fields of the $CaCO_3$ polymorphs (calcite I, calcite II, aragonite). The studies were aimed at ascertaining whether the different types of preferred orientation produced in the deformed aggregates gave any indication as to which of the known deformation mechanisms could have been active under the experimental conditions. The deformation mechanisms in calcite are well known as a result of the optical studies of deformed calcite single crystals and Yule marble [2–4].

Because of the small grain-size of the aggregates used in the new experiments, optical investigation of the microstructure in the individual grains of calcite in the deformed limestones is not possible. The additional resolution afforded by electron microscopy must be utilized to obtain information about intragranular processes. This approach has been made possible by recent advances in specimen preparation methods for minerals and aided by the advent of the high-voltage electron microscope. At present the electron microscope studies are in an early stage and we are only able to present rather general descriptions of the samples.

2. Experimental

The starting material for all the test samples described here was Solnhofen limestone (Upper Jurassic, Bavaria) which is an impure calcite lithographic limestone, with quartz and clay impurities. The limestone is extremely homogeneous with the *c*-axes lying preferentially in the bedding plane. Test samples in the form of cylinders (5 mm in diameter, 20 mm long) were cut so that the axis of compression was approxi-

mately normal to the plane of bedding. They were deformed in a piston-cylinder deformation apparatus of the type described by Griggs [5], which uses a solid confining-pressure medium (talc, in these experiments). All the samples were subjected to uniaxial compression at a constant strain rate (10^{-4} to 10^{-7}% sec^{-1}) at temperatures in the range 200 to 1000°C. For further experimental details, the reader is referred to [1].

After the compression tests, the cylinders were sectioned longitudinally. One half was used for X-ray analysis, the other half for electron microscopy. Sections were ground down to approximately 30 μm thickness. Suitable pieces, approximately 2 × 2 mm, were usually cut from the centre of the demounted polished sections and glued to thick slot-type copper electron-microscope grids with epoxy cement so that the direction of the compression axis was known. Limestones thus mounted were then prepared for TEM by ion-thinning, as described by Barber [6]. Carbonates are somewhat prone to radiation damage by the Ar^+ ions used for sputter-thinning; point-defect clusters and thin amorphous surface layers are the results. To keep these effects to an acceptable minimum it was necessary to restrict ion energies to 5.5 keV or less, to use low ion-current densities ($\lesssim$ 1 μA mm^{-2}) and to perform the final stages of thinning at $\sim$ 11° glancing angle. The limestone foils were examined at 100 keV, and at 1 MeV using the high-voltage electron microscope at Imperial College, London. The 1 MeV electron beam slowly produces radiation damage in limestones and care must be taken if this is to be kept to a minimum. However, the additional penetration afforded by working at 1 MeV was found to be highly advantageous.

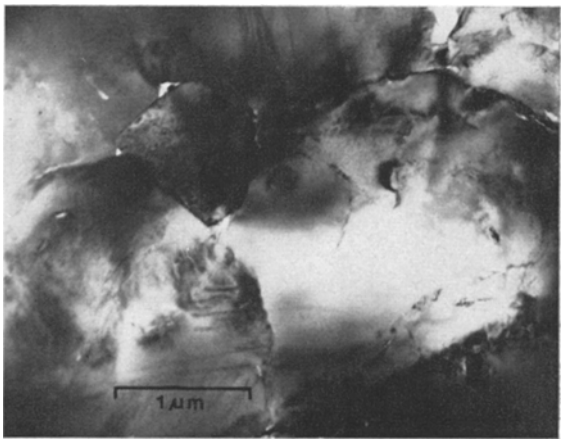

Figure 1 Untested Solnhofen limestone showing a small amount of porosity and a low density of dislocations; 100 kV.

3. Results

The undeformed limestone, which has a grain size of approximately 5 μm, is revealed in the electron microscope as a mixture of unstrained relatively dislocation-free grains and other grains containing irregular networks and sub-boundaries. There is considerable porosity, both inter- and intragranular, and there is also unidentified detritus between the grains. The electron micrograph of Fig. 1 is a fairly typical field of view.

The deformed specimens which have so far been studied by TEM are listed in Table I, which also gives the conditions of test. For the results of X-ray investigations on these and other limestones, the reader is again referred to Wenk and Venkitasubramanyan [1]. We discuss the eight specimens in order of increasing tempera-

TABLE I

Specimen number	Confining pressure (kbar)	Temperature (°C)	Log strain-rate (% sec^{-1})	% shortening	Grain size (μm)	Main phase Ca = Calcite Ar = Aragonite
GB 140	9.5	200	4	26	4–8	Ca
GB 101	9.7	300	4	28	8–12	Ca
GB 104	15	500	5	30	13–32	Ar
GB 105	15	600	5	32	up to 200	Ar
GB 121	14.7	600	6	36	up to 1000	Ar
GB 109	15	700	5	32	16–25	Ca + Ar
GB 68	11	900	4	44	35–50	Ca
GB 154	12	1000	4	53	32–50	Ca

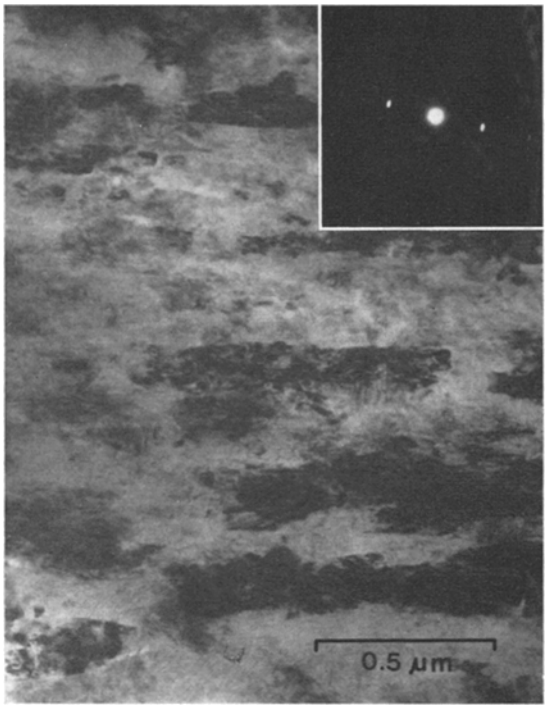

Figure 2 Heavy deformation on distorted planes in calcite (limestone GB 140), strained at 200°C. The electron diffraction spots are arced; 1 mV.

ture since temperature has the largest effect on the microstructure.

It can be seen from Table I that the test conditions for GB 101 and GB 140 are comparable in all but the temperature. TEM shows that both specimens are very heavily worked, with very high densities of dislocations in most grains and a large amount of cracking. In particular GB 140 is highly disrupted, as illustrated by Fig. 2. The grain size is essentially that of the undeformed limestone and the electron diffraction patterns correspond to calcite. However, the limestone is broken up into small sub-cells by extremely ragged faults, which although they traverse a distorted and cracked fabric exhibit a rough alignment. These faults, whose exact nature somewhat defies analysis because of the unresolvable defects within them, clearly represent "planes" where the deformation has been concentrated. The situation is somewhat less complex in GB 101, for although the ragged faults are still numerous, they are more continuous, cracking is less severe and individual dislocations within slip structures can be resolved because their strain fields do not interfere so badly. Moreover, for the first time there is evidence of fine straight faults cutting through the complex tangles of dislocations. These straight faults are deformation twins and are shown in Fig. 3. They become more profuse as the testing temperature increases, as we shall show. We believe that the ragged distorted faults which predominate in GB 140 and 101 are presumably the manifestation of what geologists refer to as translation gliding on $r\{10\bar{1}4\}$, (Bravais indices)*. The fault traces are consistent with the intersection of planes of the type $\{10\bar{1}l\}$ with the reciprocal lattice sections of the diffraction pattern, although the distortions make precise analysis impossible.

From the microstructures of GB 104 and 105 (for both of which X-ray studies show that conversion to aragonite has largely occurred during the experiments), it must be concluded that there is sufficient mobility of point defects for climb to occur at 500°C and above. Dislocation densities are in general somewhat lower than in GB 101, complex tangles are absent, there are long segments of dislocation in some grains and pieces of irregular dislocation network can be found. There is an increase in grain size as compared with the low temperature samples. Most of the calcite grains which still occur amongst the aragonite are traversed by

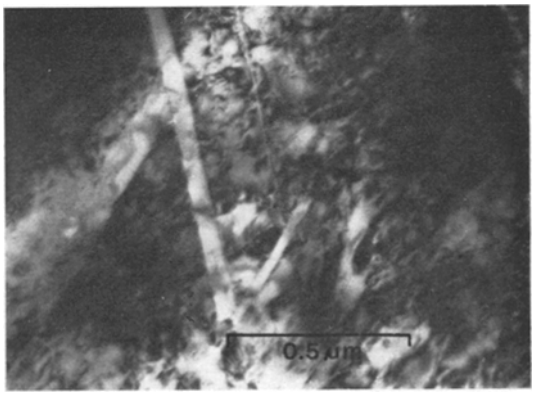

Figure 3 Narrow twin bands cutting through heavily deformed calcite grain in GB 101, strained at 300°C; 100 kV.

*In discussing calcite, we use the X-ray smallest cell (hexagonal) with $c = 17.061$ Å and $a = 4.990$ Å. Thus translation gliding and twinning on r $\{10\bar{1}1\}$ and $e\{01\bar{1}2\}$, respectively, in the cleavage rhomb cell become $r\{10\bar{1}4\}$ and $e\{01\bar{1}8\}$ in the X-ray cell.

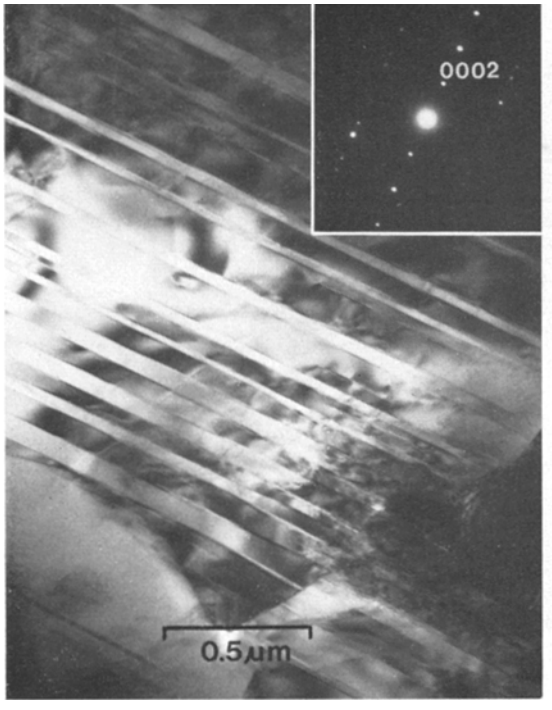

Figure 4 Fine twinning of calcite in limestone GB 105, strained at 600°C. Note the straight twin boundaries, which intersect the foil plane in the same line as the {0002} planes, which give the strong first order reflection in the diffraction pattern; 1 mV.

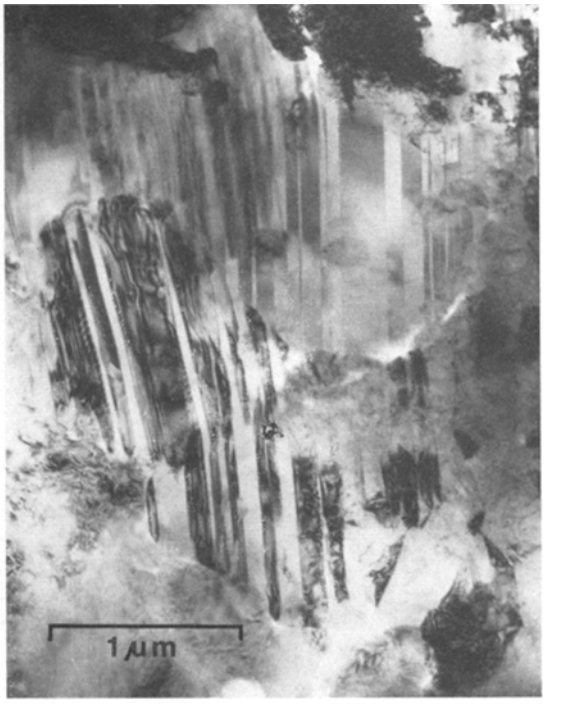

Figure 5 Three adjacent calcite grains which exhibit substantial alignment of twins, which is allied to the preferred orientation in the limestone after testing at 600°C (GB 105); 1 mV.

well-formed twins and there is a degree of twin alignment from grain to grain, indicative of the preferred orientation which has already been established by X-ray determination of pole-figures [1]. Fig. 4 shows a twinned calcite grain with its corresponding area diffraction pattern containing the prominent 0002 spacing. On tilting such a grain, the contrast can be reversed and it is observed that the crystal matrix on both sides of the twin boundaries is dislocated. We thus believe that the observed twinning is merely a development of the thin twin-gliding lamellae which have been found cutting through cold-worked grains in GB 101. Analysis of the data obtained to date shows that the fault plane is of the type $\{10\bar{1}l\}$, which would be consistent with *e*, $\{01\bar{1}8\}$, the twin plane in calcite.† Tilting experiments aimed at removing the ambiguity in l due to unknown foil thickness will be performed as soon as possible. The "clean" appearance of the faults and the ability of the regions on either side of a fault to be made to diffract strongly in turn on tilting suggests that the faults are indeed deformation twins. Fig. 5 which is also of calcite in GB 105 demonstrates clearly the rough alignment of twins in adjacent grains, referred to above as indicative of preferred orientation.

The identification of aragonite and calcite in these samples is not such a simple matter as might be anticipated, because both phases contain large numbers of planar faults. But we have come to recognize characteristics of the images of the fault boundaries in the electron microscope which are some guide in phase identification when electron diffraction is not definitive (both aragonite and calcite have many reflections many of which have closely similar d^* values). The calcite grains can usually be tilted into an orientation where the twins appear clearly as beautifully straight ostensibly parallel faults, free from complex fringes in the twin boundaries. The aragonite in these samples tested at medium temperatures tends to be very distorted so that the faults within it cannot usually be made to

†It is usually not possible to distinguish positive and negative axes by electron diffraction.

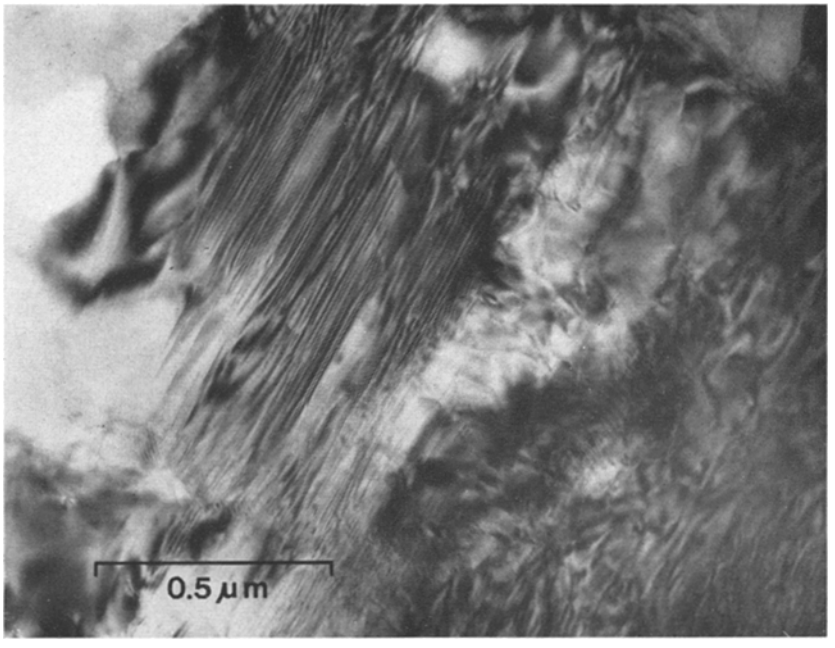

Figure 6 Complex contrast effects caused by planar faults and dislocations in aragonite in limestone strained at 600°C (GB 105); 1 mV.

diffract uniformly along their whole length. Thus the faults appear as complex sets of fringes which are in strong contrast in certain patches within the aragonite grains. A fairly typical field of view is shown in Fig. 6. The nature of these faults is not known and it is quite probable that thay are intimately related to the calcite–aragonite transformation. However, none of the diffraction patterns from these aragonite grains have so far shown the presence of calcite reflections. If residual calcite is interlamellar with the aragonite, as we would expect if the phase transformation were martensitic, then we have failed to recognize it. From comparison of fault images and diffraction patterns the fault plane has been found to be of the type $\{10l\}$ where l is either 1, 2 or 3. The ambiguity can be removed by tilting experiments, but these have not been a part of the preliminary survey.

Glassy lozenge-shaped regions which are often cracked transversely have also been seen in GB 104 and 105. It is probable that these non-crystalline regions are "foreign" matter originally present in the Solnhofen limestone rather than a phase transformed from the crystalline state by deformation. The cracking may well be an unloading effect.

Specimen GB 121, which like GB 105 was also tested at 600°C, shows rather more frequent twinning in the calcite grains but the dislocation densities are comparable. The aragonite grains are again heavily faulted and, of course, predominate in number. But the structures in the calcite are more amenable to interpretation at present. Chevron-like structures occur in a number of the calcite grains and occasionally the line of the apices is decorated with voids. The faults in the calcite appear to be of two types: one type is clearly related to the ragged structures seen in the cold-worked specimens, GB 140 and 101; they are deformation bands in heavily deformed grains. The other principal form of defect occurs in grains which have lower dislocation densities and has previously been described as deformation-twinning.

In GB 109 the dislocation densities are still fairly high, the dislocation configurations are primarily deformational rather than annealing and the twins crossing the dislocated calcite grains are still in evidence, although not so closely spaced. The twin bands are now sufficiently broad to be seen quite clearly in the polarizing microscope; Fig. 7 shows part of an ion-thinned foil. It is not until we come to GB 68, which corresponds to a temperature of 900°C, that the numbers of dislocations within the twins begin to decrease significantly. Fig. 8 shows calcite in which the heavy deformation bands,

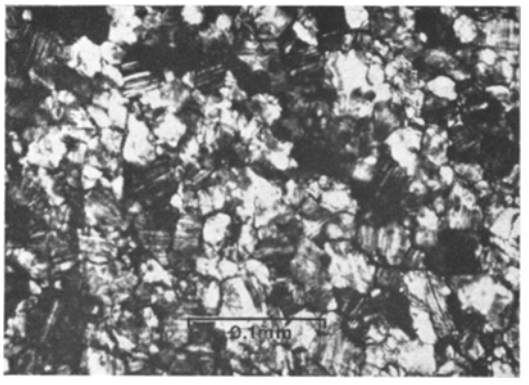

Figure 7 Transmission optical micrograph (polarized light) of part of thinned foil of limestone tested at 700°C (GB 109) showing the extent and the scale of faulting in the grains.

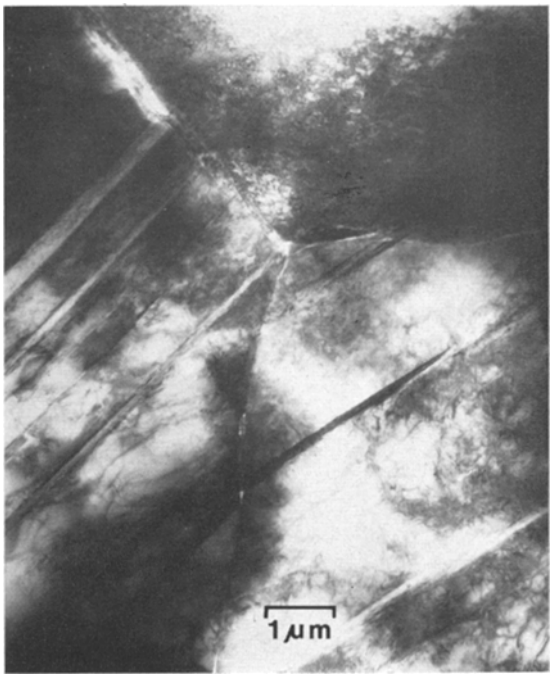

Figure 8 Heavy deformation bands with gliding dislocations and dipoles in calcite from limestone tested at 700°C (GB 109). There are many small loops which appear to be debris created during slip. The prominent first order reflection is $10\bar{1}4$; 1 mV.

with glide dislocations trailing from them, are more or less evenly spaced. The diffraction pattern indicates that the bands are parallel to $\{10\bar{1}l\}$. The smallest strain centres and loops visible in this figure were seen to be forming in the microscope and some of the dislocations were also slightly mobile. These small defects are probably the manifestation of radiation damage or could just be the aggregation of jog-induced point defects by electron beam heating.

The structures within the aragonite in GB 109 do not appear markedly different from those described for GB 104 and 105. Much more effort will have to be devoted to their analysis before we can explain their nature and origins.

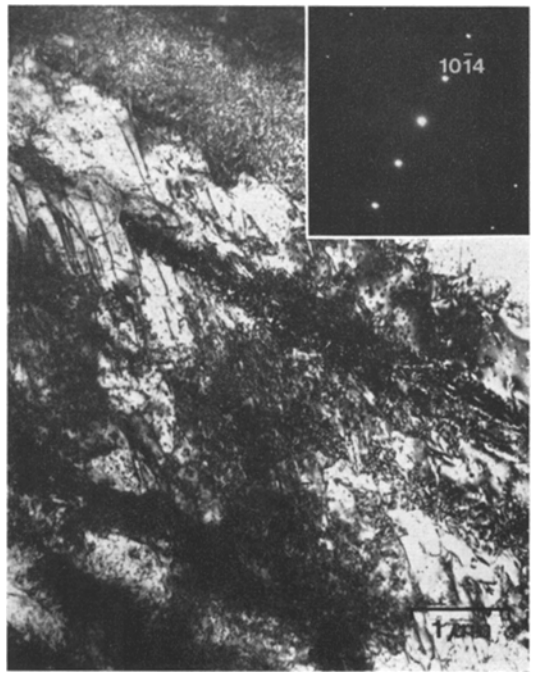

Figure 9 Slip and twinning in limestone strained at 900°C (GB 68), showing cracks opening up along the grain boundaries; 1 mV.

No evidence has been found for the existence of aragonite in either GB 68 or 154, in agreement with the X-ray studies. Somewhat surprisingly, deformation structures are still quite complex and in untwinned grains high densities of glide dislocations can still be found. Fig. 9 shows the junction between three grains in GB 68, two of which are twinned. Note that the twin lamellae are much less densely spaced than in Fig. 4, and that the grain boundaries are tending to open up. At this magnification the slip dislocations in the lower untwinned grain are hardly resolvable but they are well illustrated in Fig. 10, which is from GB 154. Here the slip direction is quite apparent and many of the

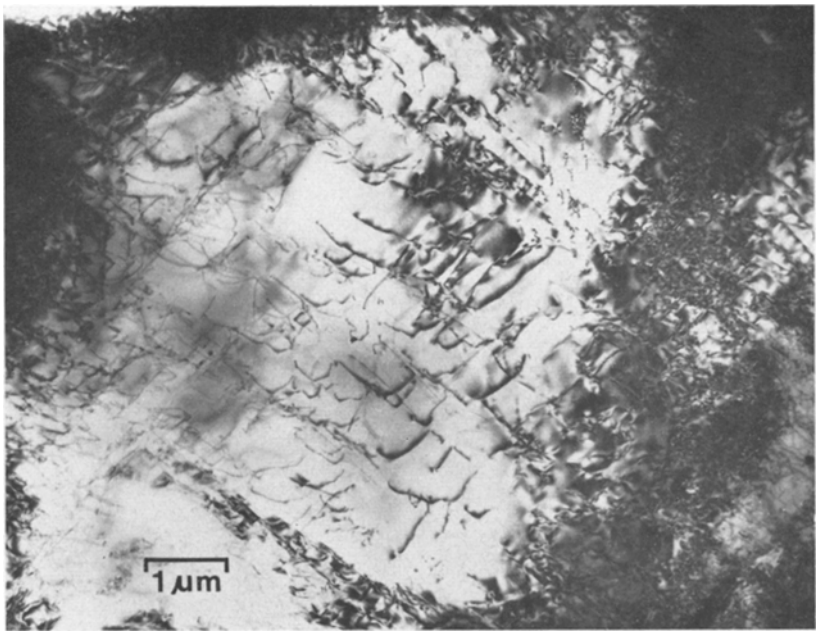

Figure 10 Intersecting glide dislocations in calcite grain from limestone tested at 1000° C (GB 154); 1 mV.

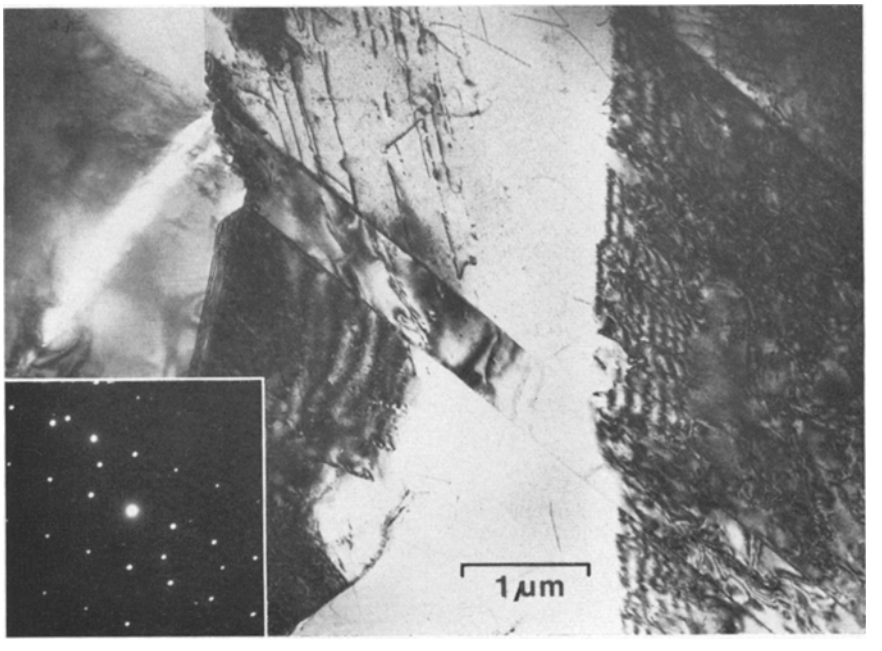

Figure 11 Twin lathe cutting through pre-existing substructure in calcite from sample strained at 900° C (GB68). There is porosity where the twin meets the grain boundary; note also the glide dislocations and dipoles; 1 mV.

advancing dislocations are seen to be interacting and cutting each other. In the twinned grains, slip is generally less in evidence and one can find cases where twins cut through subgrain boundaries and other structures which were probably formed at an earlier stage of deformation. Fig. 11 illustrates behaviour of this type in GB 68, the serrated fringes denote the position

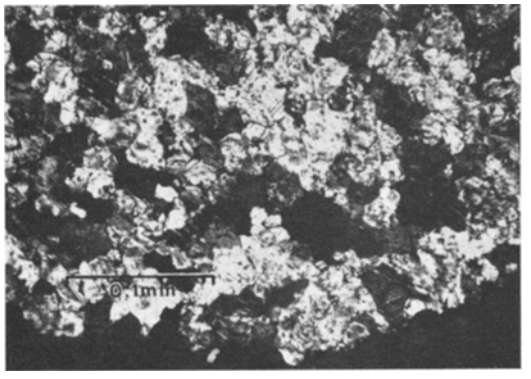

Figure 12 Transmission optical micrograph (polarized light) of part of thinned foil of limestone tested at 1000°C (GB 154) showing widely spaced twins.

of the subgrain boundary. Where the twin meets a grain boundary there is porosity, while slip dislocations and dipoles are also apparent.

The trend towards simpler structures which is evident in GB 109 is carried a stage further in GB 154. The tendency for networks to form is more pronounced and the density of twins is lower. This is, of course, apparent even in the polarizing microscope as shown by Fig. 12. Fig. 13 is an electron micrograph of one of the twinned calcite grains; the dislocations form a loose irregular three-dimensional network. At higher magnifications one can discern that the dislocations clearly originate from glide. In Fig. 14 a number of dipoles and small pinched-off loops are visible but there is a marked tendency for crystallographic alignment and the intersections are leading to the formation of a net. The central dark feature is an impurity particle.

4. Conclusions

At the present state of the work it is not possible to interpret all these observations. Especially, the phase transition from calcite to aragonite remains a puzzle. Our ability to explain it has been hindered because of initial difficulties in distinguishing calcite from aragonite in the electron micrographs, since both minerals show somewhat similar dislocation and fault patterns.

Yet there are some significant trends which can already be interpreted: increase in temperature produces simpler structures. The dislocation den-

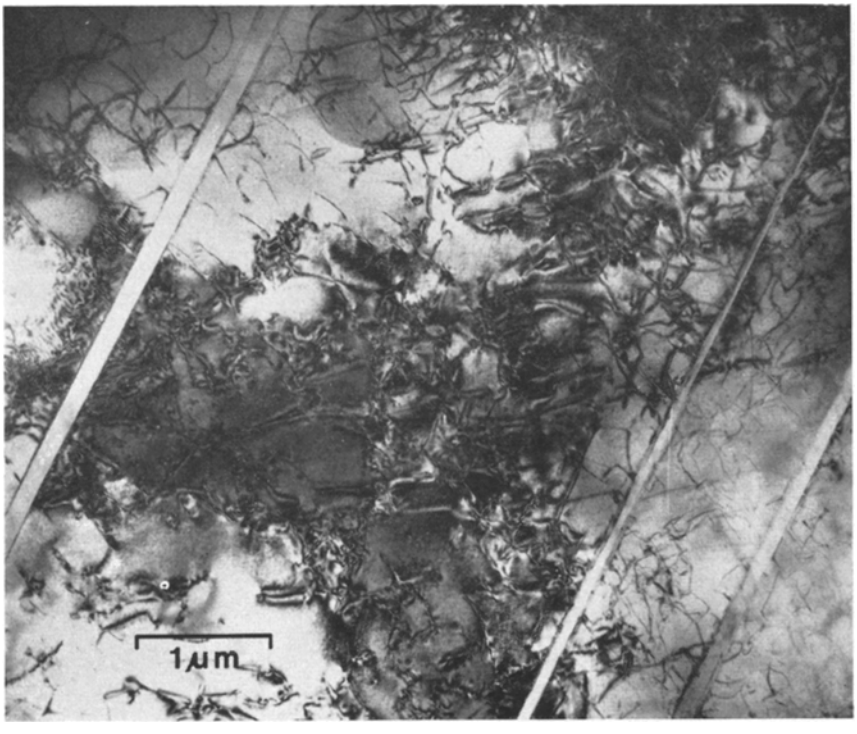

Figure 13 Widely-spaced twin bands and climbing glide dislocations in limestone strained at 1000°C (GB 154); 1mV.

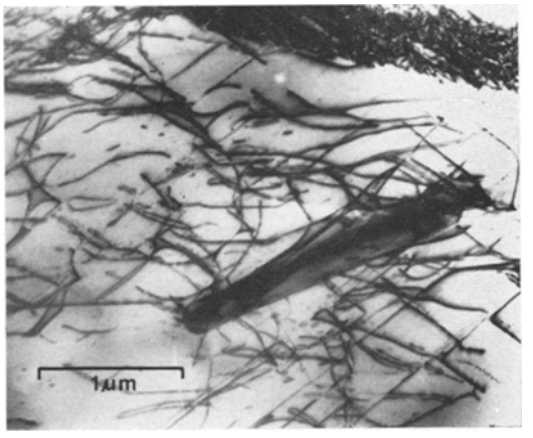

Figure 14 Dipoles and intersecting glide dislocations close to a particle of second phase in calcite grain from limestone tested at 1000°C (GB 154). 1 mV.

sity decreases and faulting is less profuse. This is in agreement with the interpretation of the pattern of preferred orientation [1]. At low temperatures translation gliding on $\{10\bar{1}4\} = r$ is very common and is combined with twin gliding on $\{01\bar{1}8\} = e$. It appears as if slip is easier at the higher temperatures and there is less need for twinnng as a mechanism of stress-relief. This may simply be a result of cross slip and climb being easier so that recovery begins and less complicated structures are the consequence. At high temperatures when recovery is competitive with the deformation process the crystals look "cleaner", with networks forming and without many fault planes. It should be noted that the observations in limestone have similarities to processes in some soft metals and they can be interpreted by analogy.

It appears that transmission electron microscopy (TEM) is a very useful method for characterizing the temperature conditions of a deformation process as has already been demonstrated for other minerals by McLaren *et al* [7]. These preliminary descriptions of the substructures in experimentally deformed limestone may help in deriving the geological conditions of deformation of natural limestones from their electron micrographs.

Acknowledgements

H.R.W. wishes to thank NSF for grants GA-1671 and GA-29294. The experiments described in this paper were done at the Institute of Geophysics and Planetary Physics at UCLA. We acknowledge the generosity of D. T. Griggs and J. M. Christie (NSF grants GA-1389 and GA-26027) for giving us the opportunity to use their laboratory. We also wish to thank P. R. Swann for his most valuable help in making available to us the EM7 1 MeV electron microscope at Imperial College, London.

References

1. H. R. WENK and C. S. VENKITASUBRAMANYAN, *Contrib. Mineral. Petrol.* (1972) in press.
2. D. T. GRIGGS, F. J. TURNER, and H. C. HEARD, *Geol. Soc. Amer. Mem.* **79** (1960) 41.
3. F. J. TURNER, D. T. GRIGGS, R. H. CLARK, and R. DIXON, *Geol. Soc. Amer. Bull.* **67** (1956) 1259.
4. F. J. TURNER, D. T. GRIGGS, and H. C. HEARD, *ibid* **65** (1954) 883.
5. D. T. GRIGGS, *Geophys. J. Royal Astron. Soc.* **14** (1967) 19.
6. D. J. BARBER, *J. Mater. Sci.* **5** (1970) 1.
7. A. C. MCLAREN, J. A. RETCHFORD, D. T. GRIGGS, and J. M. CHRISTIE, *Phys. Stat. Sol.* **19** (1967) 631.

Received 12 September and accepted 20 November 1972.